Supporting Information

Kemen et al. 10.1073/pnas.1401553111

SI Materials and Methods

Assessment of Root Length and Metabolite Analysis. Root lengths of *Avena strigosa* seedlings grown on 1% distilled water agar plates maintained vertically upright in a growth chamber at 22 °C (16-h light/8-h dark photoperiod) were measured from scanned images using Image J after 15 d of growth. For β-amyrin feeding experiments, seeds of *A. strigosa* wild-type and saponin-deficient 1 (*Sad1*) mutant lines were germinated on distilled water agar plates containing 50 or 100 μM β-amyrin (stock solution of 10 mM made in methanol; control plates contained an equivalent amount of methanol alone) and were grown at 22 °C with a 16-h light/8-h dark photoperiod for 7 d. For metabolite analysis roots were excised from 11-d-old seedlings and extracted with 75% (vol/vol) methanol at 4 °C overnight with shaking. Extracts were analyzed by LC-MS as described previously (1).

Transgenic rice lines #21 and #22 expressing oat β-amyrin synthase (SAD1) under the control of the maize ubiquitin promoter (2) were grown on GM medium (3). Root lengths were measured after 8 d. Roots also were examined at higher resolution by cryo-scanning electron microscopy (cryo-SEM) after 4 d (see below).

Plant Transformation. Promoter-deletion constructs were introduced into *Arabidopsis thaliana* Col0 plants by *Agrobacterium tumefaciens*-mediated transformation, and stable transformants were selected on hygromycin-containing plates. At least four independent lines per construct were used for analysis of reporter gene expression. Construct pHGWFSBAS2992, comprising 2,992 bp of the *Sad1* promoter region, was introduced into rice variety Nipponbare using the method described by Vain et al. (4). The same construct was used for hairy root transformation of *Medicago truncatula* using *Agrobacterium rhizogenes* ARQUA1 (5). To investigate promoter activity during nodule formation, transformed *M. truncatula* roots were infected with *Sinorhizobium meliloti* as described by Marsh et al. (6).

Microscopy. ***Analysis of β-Glucuronidase expression.*** For detection of β-glucuronidase (GUS) activity, seedlings were fixed in 90% ice-cold acetone and rinsed with 3 mM potassium ferrocyanide, 50 mM NaPO4 (pH 7). Then they were stained in 1 mM 5-bromo-4-chloro-3-indoyl glucuronide [in 3 mM potassium ferrocyanide, 50 mM NaPO4 (pH 7)] at 37 °C overnight followed by serial washing steps from 10–70% (vol/vol) ethanol. GUS-stained roots were embedded in Technovit 7100 resin (Heraeus Kulzer GmbH). Sections (10 μm) were prepared using an ultramicrotome (Ultracut E, Reichert-Jung) and examined using a Leica Axiophot microscope.

Fluorescence microscopy. GFP fluorescence was detected using a Leica SP5 confocal microscope [Leica Microsystems (UK) Ltd.] with a 488-nm laser for excitation and a BP 500- to 530-nm filter for emission. Avenacin A-1 fluorescence was imaged using a Leica Axiophot microscope (363-nm excitation, 450- to 465-nm emission) as previously described (7). Images were processed with ImageJ and assembled using Adobe Photoshop CS4.

Cryo-SEM. Roots of 2- to 4-d-old *A. strigosa* or rice seedlings were mounted horizontally on the specimen holder using a thin layer of OCT compound (BDH Laboratory Supplies). Samples then were plunged into liquid nitrogen slush at approximately −210 °C and were transferred to the cryo-stage of a CT1500HF cryo-transfer system (Gatan) attached to an FEI XL30 FEG scanning electron microscope (FEI UK Ltd). The temperature was raised to −95 °C to sublime the surface ice for 3 min and then was cooled immediately to below −110 °C before sputter coating with platinum for ∼150 s at 10 mA. After sputter coating, samples were moved onto the cryo-stage in the main chamber of the microscope, held at approximately −145 °C, and viewed at 3 kV.

RNA Extraction. Sections of 1 mm were taken from the root tips and from the maturation zone of *A. strigosa* seedlings. Fifty seedlings were used per extraction, with three biological replicates for each treatment. RNA was extracted using either TRI reagent (Sigma), followed by phenol/chloroform purification and selective precipitation with sodium acetate or an RNAeasy Plant Mini Kit (Qiagen). After DNase I (Roche) digestion, first-strand cDNA synthesis was performed with SuperScript III RT (Invitrogen) using 4–10 μg of total RNA. Quantitative RT-PCR (qRT-PCR) and relative quantification were performed as previously described (8) using either an Opticon instrument (MJ Research) or a Bio-Rad CFX96 real-time PCR detection system/C1000 thermal cycler.

Transcriptome Analysis. mRNA was extracted from the terminal 0.5 cm of the root tips of 3-d-old *A. strigosa* seedlings germinated on distilled water agar. RNA was extracted using TRIzol reagent (Life Technologies) and was purified using an Oligotex mRNA minikit (Qiagen). A combination of zinc chloride and heat was used to fragment the mRNA, and then first-and second-round cDNA synthesis was carried out using the Roche cDNA synthesis kit (with random hexamer primers). 454-Specific adapters were ligated to the cDNA, which then was size-selected according to the 454 rapid library protocol. This library was quantified using qPCR and subjected to a full-scale emulsion-based CR to generate templated beads for sequencing on the 454 platform. Massively parallel pyrosequencing was undertaken using 454 titanium chemistry (Roche) to generate more than 600 Mbp of sequence reads. Individual reads were processed through Newbler to enable transcript assembly. Transcripts corresponding to previously characterized avenacin biosynthetic genes were identified within this contig collection. Each of the five contigs identified contained the full-length coding sequence (CDS) plus flanking 5′ and 3′ UTR sequences (Table S1). The 454 contig collection then was mined for class IV homeodomain leucine zipper (HD-ZIP IV) family members that were identified through BLAST (tBLASTn) searches using all 16 *A. thaliana* HD-ZIP IV family members. We identified 101 reads corresponding to a single contig (c04446).

Subcloning of *AsHDZ1*. The complete coding sequence of *AsHDZ1* was amplified from cDNA using the primers listed in Table S2. *AsHDZ1* was subcloned using the pENTR Directional TOPO Cloning Kit (Invitrogen).

Phylogenetic Analysis. Amino acid sequences from HD-ZIP IV family members from the monocots *Brachypodium* (Bd), wheat (Ta), barley (Hv), rice (Os), maize (Zm), and *Aegilops* (Aet) and from the eudicots *A. thaliana* (At) and grape (Vv) were obtained from National Center for Biotechnology Information (NCBI). The names in the phylogenetic tree correspond to the NCBI identification numbers. Sequences for poplar were obtained from table S2 of Hu et al. (9). *M. truncatula* (Medtr) sequences were downloaded from the NCBI and HAPMAP (www.medicagohapmap.org/) databases. HD-ZIP proteins from *Physcomitrella patens* (Pp) were downloaded from (www.uniprot.org/).

The HD-ZIP family IV sequences were aligned using ClustalW2 (10). The maximum likelihood (11) phylogenetic tree was generated based on a gap-free alignment with 1,000 replicates of bootstrap analysis. The unrooted phylogenetic tree was displayed using FigTree (v1.4.0) (http://tree.bio.ed.ac.uk/software/figtree).

1. Mugford ST, et al. (2009) A serine carboxypeptidase-like acyltransferase is required for synthesis of antimicrobial compounds and disease resistance in oats. *Plant Cell* 21(8):2473–2484.
2. Inagaki Y-S, et al. (2011) Investigation of the potential for triterpene synthesis in rice through genome mining and metabolic engineering. *New Phytol* 191(2): 432–448.
3. Valvekens D, et al. (1988) Agrobacterium tumefaciens-mediated transformation of Arabidopsis thaliana root explants by using kanamaycin selection. *Proc Natl Acad Sci USA* 85(15):5536–5540.
4. Vain P, Afolabi AS, Worland B, Snape JW (2003) Transgene behaviour in populations of rice plants transformed using a new dual binary vector system: pGreen/pSoup. *Theor Appl Genet* 107(2):210–217.
5. Boisson-Dernier A, et al. (2001) *Agrobacterium rhizogenes*-transformed roots of *Medicago truncatula* for the study of nitrogen-fixing and endomycorrhizal symbiotic associations. *Mol Plant Microbe Interact* 14(6):695–700.
6. Marsh JF, et al. (2007) Medicago truncatula NIN is essential for rhizobial-independent nodule organogenesis induced by autoactive calcium/calmodulin-dependent protein kinase. *Plant Physiol* 144(1):324–335.
7. Osbourn AE, Clarke BR, Lunness P, Scott PR, Daniels MJ (1994) An oat species lacking avenacin is susceptible to infection by *Gaeumannomyces graminis* var. *tritici*. *Physiol Mol Plant Pathol* 45(6):457–467.
8. Livak KJ, Schmittgen TD (2001) Analysis of relative gene expression data using real-time quantitative PCR and the 2(-delta delta C(T)) method. *Methods* 25(4):402–408.
9. Hu R, et al. (2012) Genome-wide identification, evolutionary expansion, and expression profile of homeodomain-leucine zipper gene family in poplar (*Populus trichocarpa*). *PLoS ONE* 7(2):e31149.
10. Larkin MA, et al. (2007) ClustalW and ClustalX version 2. *Bioinformatics* 23(21): 2947–2948.
11. Felsenstein J (1981) Evolutionary trees from DNA sequences: a maximum likelihood approach. *J Mol Evol* 17(6):368–376.

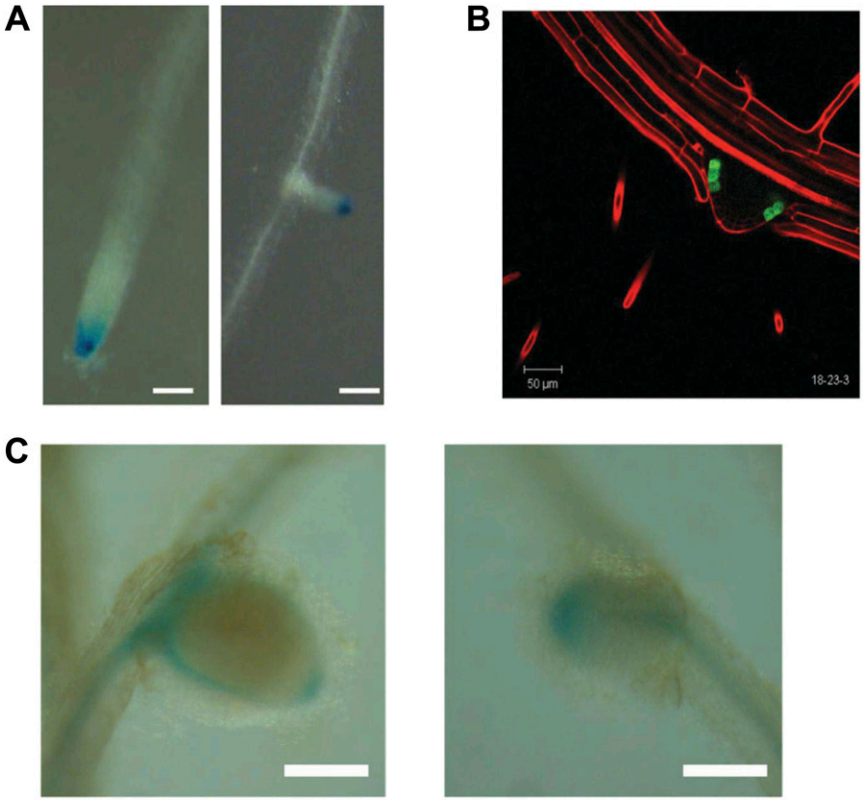

Fig. S1. (*A*) Staining for *Sad2* promoter (*pSad2*)-driven GUS expression in *A. thaliana*. (Scale bars: 100 µm.) (*B*) Sad1 promoter (*pSad1*)-driven GFP expression in an emerging lateral root in *A. thaliana*. (Scale bar: 50 µm.) (*C*) *pSad1*-driven GUS expression in nodules of *M. truncatula*. (Scale bar: 200 µm.)

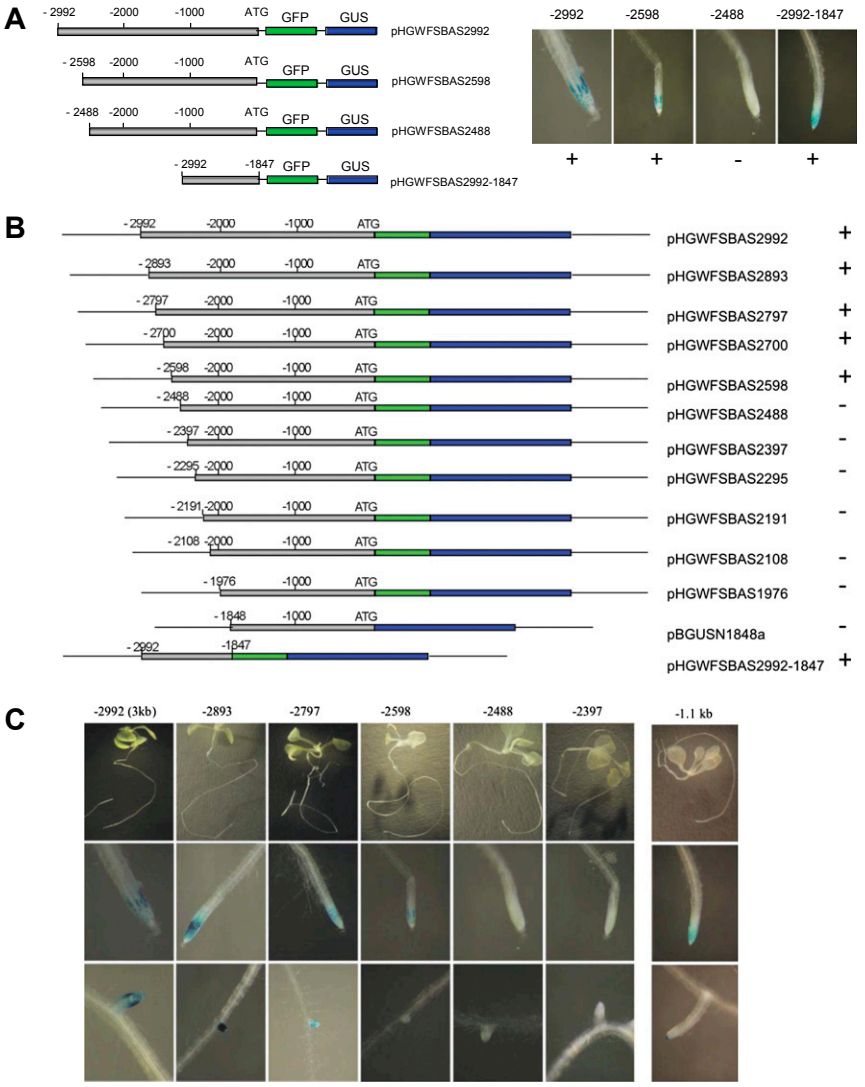

Fig. S2. Preliminary deletion analysis of the *pSad1* promoter. (*A*) Initial deletion series. (*Left*) Promoter fragments (gray) are fused to the coding region of GFP (green) and GUS (blue). Numbers indicate nucleotide positions relative to the translation start codon ATG. (*Right*) Results of GUS staining: +, positively stained; −, clearly reduced or absent GUS staining. (*B*) Fine deletion series. (*Left*) Constructs. (*Right*) Detection of GUS activity in 10 d-old *A. thaliana* seedlings is indicated by + and − scores. (*C*) GUS staining for whole seedlings (*Top Row*), primary root tips (*Middle Row*), and lateral roots (*Bottom Row*).

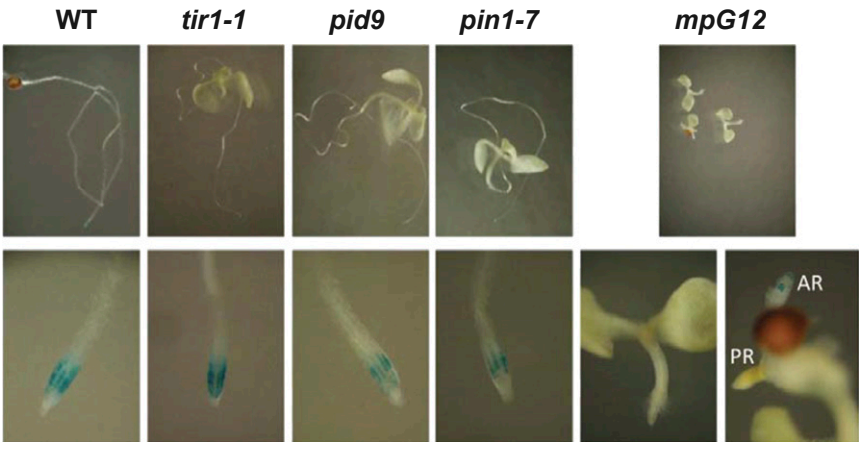

Fig. S3. *pSad1* activity is auxin independent. GUS-stained seedlings (*Upper*) and primary roots (*Lower*) of the F3 generation of the auxin mutants *tir1-1*, *pid9*, and *pin1-7* and the F2 generation of *mp12G*. AR, adventitious root; PR, primary root.

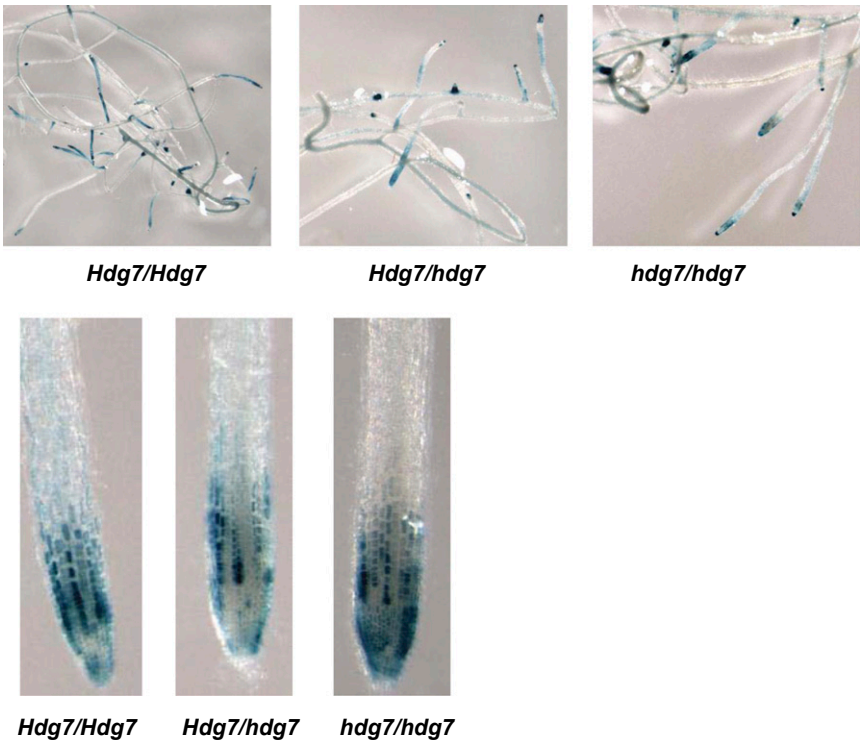

Fig. S4. *pSad1-GUS* expression is not compromised in *hdg7* mutant lines. Detection of GUS activity in 10-d-old *A. thaliana* seedlings (*Upper*) and in primary root tips (*Lower*) is shown.

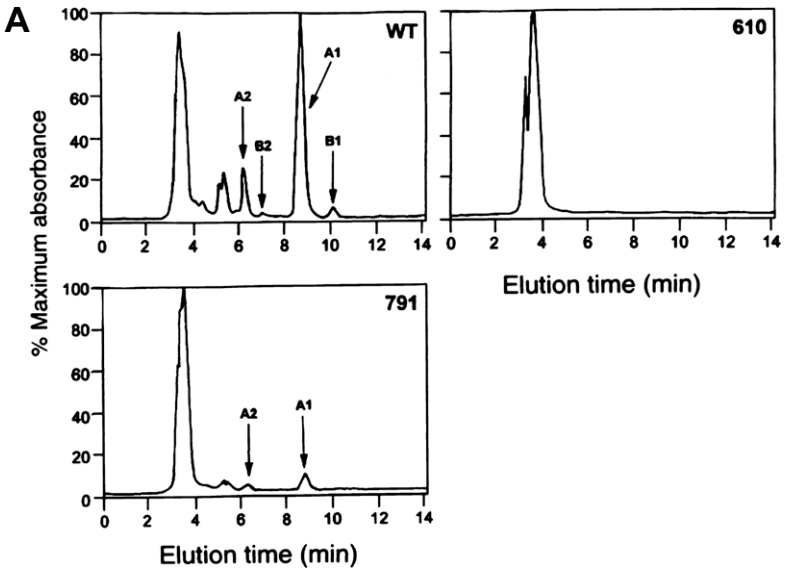

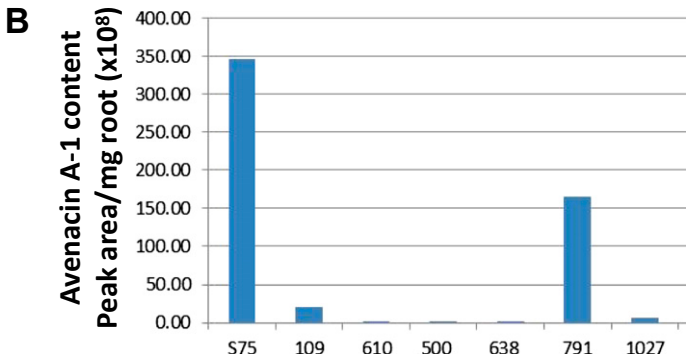

C

	Mean β-amyrin content (μg/g roots) ± s.d.	
	Experiment 1[a]	Experiment 2[b]
Wild type (S75)	1.4 ± 0.1	2.0 ± 0.0
#109 (*sad1*)	-	0.8 ± 0.0
#791 (*sad2*)	40.2 ± 1.9	38.7 ± 3.2
#1027 (*sad2*)	50.4 ± 1.2	47.7 ± 4.7

Fig. S5. Avenacin and β-amyrin content of oat lines. (*A*) HPLC analysis of crude extracts from roots of wild-type and mutant oat lines. The peaks corresponding to the four avenacins (A-1, A-2, B-1, and B-2) are indicated for extracts from wild-type roots (*Upper Left*). Extracts from mutants #109 (*sad1*), #610 (*sad1*), and #1027 (*sad2*) did not contain detectable levels of avenacins (an example of an HPLC trace for #610 is shown), whereas #791 (a partial *sad2* mutant) contained reduced levels. The full-scale deflection was 4.1 mV for the wild-type line and 5.5–8.5 mV for the mutants (data reproduced from ref. 1). (*B*) Representative LC-MS analysis of the avenacin A-1 content of roots of the *A. strigosa* wild-type strain S75 and *sad1* (#1090, #610) and *sad2* (#500, #638, #791, and #1027) mutants (see *SI Material and Methods* for details). (*C*) β-Amyrin content of roots of wild-type and *sad1* and *sad2* mutant lines [a]Data for experiment 1 are reproduced from ref. 1. [b]Data for experiment 2 are reproduced from ref. 2.

1. Papadopoulou K, Melton RE, Leggett M, Daniels MJ, Osbourn AE (1999) Compromised disease resistance in saponin-deficient plants. *Proc Natl Acad Sci USA* 96(22):12923–12928.
2. Qin B, et al. (2010) High throughput screening of mutants of oat that are defective in triterpene synthesis. *Phytochemistry* 71(11-12):1245–1252.

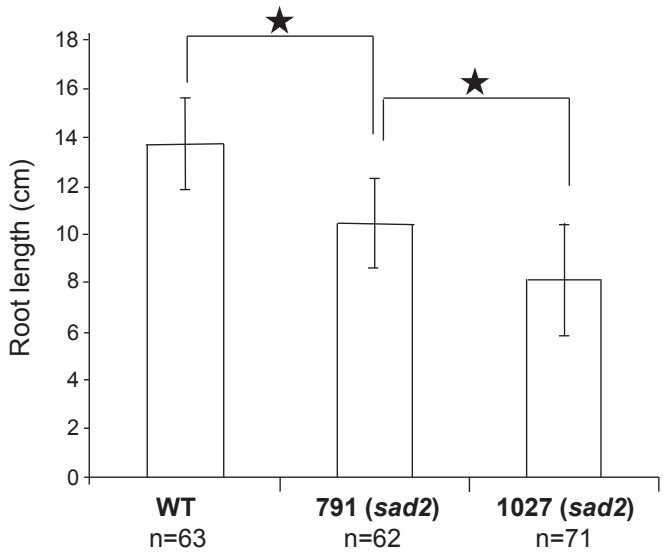

Fig. S6. Root lengths of *A. strigosa* wild-type and null (#1027) and partial (#791) *sad2* mutant lines after 15 d growth on vertical plates. Mutant #791 accumulates β-amyrin at levels that are intermediate between those of null *sad2* mutants (such as #1027) and the wild type (1, 2). Results are presented as means ± SE; *n* indicates the number of seedlings analyzed. $*P < 0.0001$ (unpaired two-tailed *t* tests).

1. Papadopoulou K, Melton RE, Leggett M, Daniels MJ, Osbourn AE (1999) Compromised disease resistance in saponin-deficient plants. *Proc Natl Acad Sci USA* 96(22):12923–12928.
2. Qi X, et al. (2006) A different function for a member of an ancient and highly conserved cytochrome P450 family: From essential sterols to plant defense. *Proc Natl Acad Sci USA* 103(49): 18848–18853.

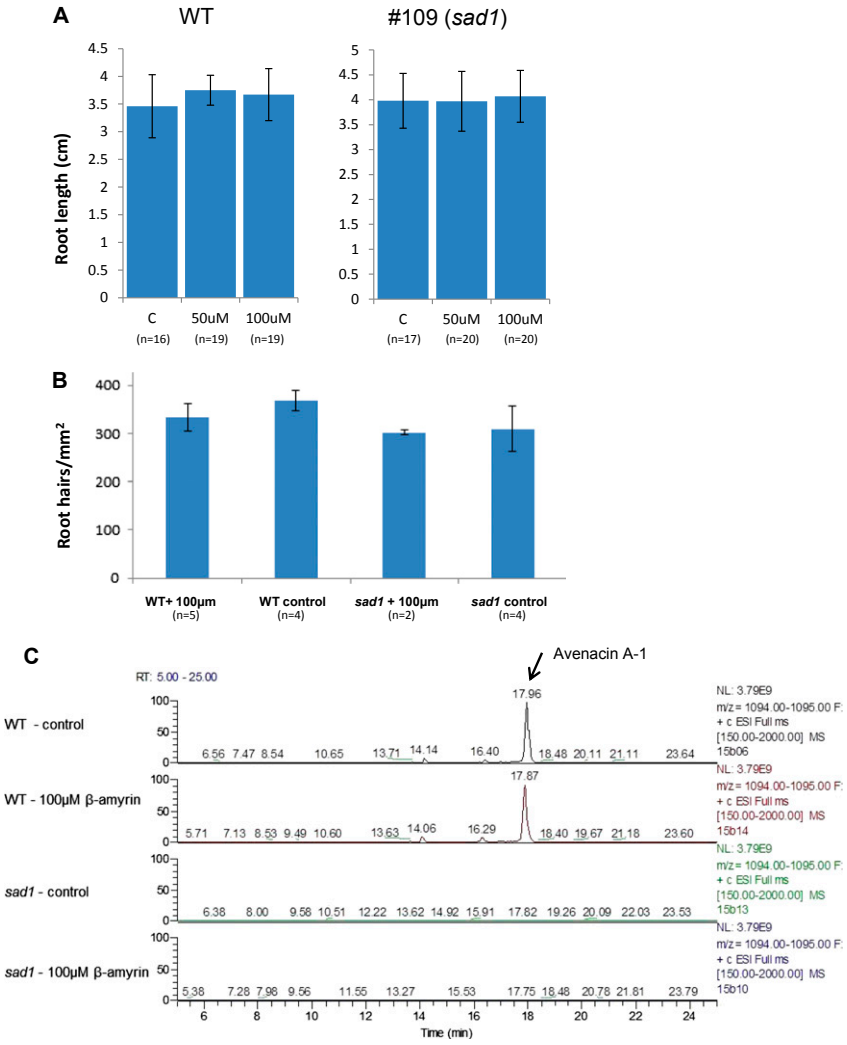

Extracted ion chromatogram for avenacin A-1 (*m/z* 1094.6)

Fig. S7. Assessment of the effects of exogenous β-amyrin on root growth of *A. strigosa* wild-type and *sad1* mutant (#109) lines. Seeds were germinated on distilled water agar containing 50 or 100 μm β-amyrin (stock solution made in methanol) or an equivalent amount of methanol as the control (C). (*A*) Root lengths, measured after 7 d [one-way ANOVA; wild type: $F(2,51) = 1.845$, $P = 0.1684$; *sad1* #109: $F(2,54) = 0.1959$, $P = 0.82267$)]. (*B*) Root hair density, measured after 4 d. Values are means ± SD; *n* indicates the number of seedlings analyzed. Wild type: $P = 0.02$, suggesting a small negative effect of β-amyrin treatment on root hair density in the wild type; *sad1* #109: $P = 0.85$ (unpaired two-tailed *t* test). (*C*) Analysis of the avenacin content of root extracts from 11-d-old seedlings by LC-MS (see *SI Materials and Methods*).

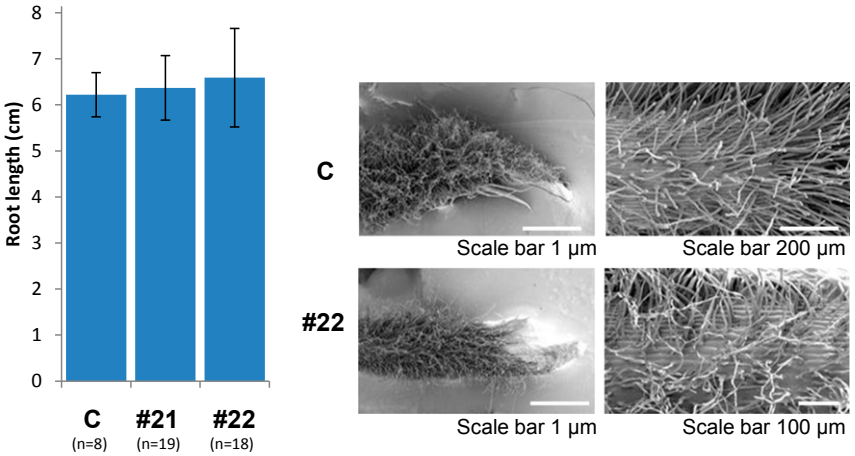

Fig. S8. Analysis of transgenic rice lines expressing SAD1 under the control of the maize ubiquitin promoter [see Inagaki et al. (1) for further information about the rice lines]. (*Left*) Root lengths in 8-d-old seedlings; means are shown for 8, 19, and 18 seedlings, respectively; error bars indicate SD [one-way ANOVA: $F(2,45) = 0.899$, $P = 0.414$)]. (*Right*) Cryo-SEM showing the appearance of the roots in 4 d-old seedlings.

1. Inagaki Y-S, et al. (2011) Investigation of the potential for triterpene synthesis in rice through genome mining and metabolic engineering. *New Phytol* 191(2):432–448.

Table S1. Contigs obtained for the *Sad* genes and *HDZ1* from 454-based transcriptomic analysis

Gene	Contig number	No. of reads	CDS size, bp	Contig size, bp
Sad1	09590	1,132	2,271	2,619
Sad2	17168	918	1,470	18,01
Sad7	25523	170	1,479	1,602
Sad9	16631	375	1,062	1,243
Sad10	07600	71	1,392	1,667
AsHDZ1	04446	101	2,394	2,995

Table S2. Primer sequences for *Sad1*, *Sad2*, and *Ubi* promoter–reporter constructs and deletion series and cloning of *AsHDZ1*

Gene	Primer	Sequence 5′–3′
Sad1	pBAS-F	GGGGACAAGTTTGTACAAAAAAGCAGGCTATGTCCCTATCTATATTTGAG
	pBAS_R	GGGGACCACTTTGTACAAGAAAGCTGGGTGCCATGGTGCCCACCAACAACG
	AS-amy1848F	GAGCTCGGATCCGATCACTGGCTACGCCGAGATTCTAC
	ASamy-P3R	GGATCCGAGCTCGAGCAATGTTCTTATTCCTCGCAGCCTAGA
	pBAS-F2893	GGGGACAAGTTTGTACAAAAAAGCAGGCTGATTTTTCTAAGATTAATGTG
	pBAS-F2797	GGGGACAAGTTTGTACAAAAAAGCAGGCTCGTTAGCCCAATGGGCTACG
	pBAS-F2700	GGGGACAAGTTTGTACAAAAAAGCAGGCTGTCAAGCTACGCCGACGGTC
	pBAS-F2598	GGGGACAAGTTTGTACAAAAAAGCAGGCTGTAACTATCCTAACCGGTAGG
	pBAS-F2488	GGGGACAAGTTTGTACAAAAAAGCAGGCTCAATATCAGATTAACCTGGG
	pBAS-F2397	GGGGACAAGTTTGTACAAAAAAGCAGGCTCTGCAAGACAAGATCCACGG
	pBAS-F2295	GGGGACAAGTTTGTACAAAAAAGCAGGCTCAACCATCGTGTATTCTGCAC
	pBAS-F2191	GGGGACAAGTTTGTACAAAAAAGCAGGCTCTTCACATGCGGTGTCTGATC
	pBAS-F2108	GGGGACAAGTTTGTACAAAAAAGCAGGCTCGTCTTATGGCCTCGAGTAC
	pBAS-F1976	GGGGACAAGTTTGTACAAAAAAGCAGGCTCTAGTGGCACTACTGAAATC
	pBAS-R1.1kb	GGGGACCACTTTGTACAAGAAAGCTGGGTGAGAGCTTTACGGAATCCG
Sad2	pCYPA-F	GGGGACAAGTTTGTACAAAAAAGCAGGCTGTGTCGATAGGGACCCATGC
	pCYPA-R	GGGGACCACTTTGTACAAGAAAGCTGGGTGCCATGTCGTTATTGACTAGAGG
Ubiquitin	pUBI-F	GGGGACAAGTTTGTACAAAAAAGCAGGCTAATGAGCATTGCATGTCTAAG
	pUBI-R	GGGGACCACTTTGTACAAGAAAGCTGGGTGCCATTGCAGAAGTAACACCAAACAAC
AsHDZ1	AsHD-ZIP-F-GW	CACCATGAGCTTTGGGGGCCTCTTTGAC
	AsHD-ZIP-R-GW	CTMACAATCAGGCATTGGGCACTG

Table S3. Primer sequences for qRT-PCR

Gene	Gene-specific primer	Sequence 5′–3′
Sad1	Sad1q-5′	TGCGGAATTCACAAAGAACA
	Sad1q-3′	GCTTGGCTTCTGTCGGAATA
CAS1	CAS1-2q-5′	CATCATGGGGAAAGTTTTGG
	CAS1-2q-3′	GTGACACCACATTCGACCTG
Sad2	Sad2q-5′	TCGACAGGAAGTGGAGGAGT
	Sad2q-3′	ATCTCGGACCTCACTTCCAA
Cyp51G1	Cyp51q-5′	ACTACCTGGTCAGGCAGGAG
	Cyp51q-3′	CCCCACGTCGAGAAGTAGTC
EF1-α	EF1aq-5′	TCCCCATCTCTGGATTTGAG
	EF1aq-3′	TCTCTTGGGCTCGTTGATCT
AsHDZ1	C04446_1-5′	GCAGCCTTCAATGCACAGTA
	C04446_1-3′	AGACGGATCTGTCGATGTCC

EF1-α, oat elongation factor1-α.